Optimization of the lattice function in the planar undulator applied for terahertz FEL oscillators

YANG Lei(杨磊) QIN Bin(秦斌)[1)] YANG Jun(杨军) LIU Xia-Ling(刘遐龄)
TAN Ping(谭萍) HU Tong-Ning(胡桐宁)

State Key Laboratory of Advanced Electromagnetic Engineering and Technology,
Huazhong University of Science and Technology, Wuhan 430074, China

Abstract: Since the beta function of the electron beam within the undulator has a great influence on the power gain of the free electron laser (FEL), optimization of the undulator lattice becomes important. In this paper, the transfer matrix of the planar undulator is obtained from differential equations of the electron motion. Based on this, the lattice function of the planar undulator in a terahertz FEL oscillator proposed by Huazhong University of Science and Technology (HUST-FEL) is optimized and the expressions of the average beta function are derived. The accuracy of the optimization result was confirmed well by the numerical method. The application range of this analytical method is given as well. At last, the emittance growth in the horizontal direction due to the attenuation of the magnetic field is discussed.

Key words: planar undulator, beam transport, lattice optimization

PACS: 41.60.Cr, 41.85.-p, 29.27.Bd **DOI:** 10.1088/1674-1137/38/3/037004

1 Introduction

Pure permanent magnet (PPM) undulators are implemented in FELs featuring a magnetostatics periodic (sinusoidal) field in the longitudinal (z) direction. Driven by the vertical magnetic field, electrons move in a sine-like orbit and interact with the stored light wave, for generating coherent radiations [1–5]. Large beta function within the undulator will enlarge the cross section of the electron beam, which leads to a decrease of the current density and finally decreases the single pass gain [6, 7]. On the other hand, too small beta function will lead to the increase of both radiation diffraction and the the equivalent energy spread derived from the betatron oscillation, that finally increases the gain length [8, 9]. Since the beta function of the electron beam in the undulator has a great influence on the gain length [7], optimization of the beta function becomes important for improving the FEL performance.

In this paper, the transfer matrices in the horizontal and vertical plane are obtained from the differential equations of the electron trajectory, which are simplified by ignoring unimportant items and using equivalent treatment. Based on the transfer matrices, the lattice functions can be obtained. As a case study, the undulator of HUST-FEL is optimized. The analyzed and optimized lattice is from 0.1 meter in front of the undulator to the place 0.1 meter behind the undulator. For validation, the results derived by numerical methods are displayed too.

The main beam and undulator parameters of HUST-FEL are listed in Table 1 [10].

Table 1. Undulator and beam parameters of HUST-FEL.

beam energy/MeV	6–12
radiation wavelength/μm	40–150
normalized emittance/(πmm·mrad)	15
micro-pulse width/ps	∼5
bunch charge/pC	∼200
energy spread (%)	0.3
undulator period/cm	3.2
undulator period number	30
peak magnetic flux density/T	0.334–0.418
undulator parameter K	1.0–1.25

2 Transfer matrix in a planar undulator

2.1 Magnetic field distribution of the planar undulator

For the analysis of beam transport characteristics, a simple approximation is taken to determine the motion of an electron in the periodic magnetostatic field of an idealized planar undulator. For the regular period, it can be shown that such a device yields a paraxial field with

Received 27 April 2013

1) E-mail: bin.qin@mail.hust.edu.cn

the following components [11]:

$$\begin{cases} B_x = B_0\delta\dfrac{k_u^2}{2}xy\sin(k_u z) \\ B_y = -B_0\left\{1+\dfrac{k_u^2}{4}[(2+\delta)y^2-\delta x^2]\right\}\sin(k_u z) \\ B_z = -B_0 k_u y\cos(k_u z) \end{cases},$$

where B_0 is the peak magnetic field value and k_u is the undulator's wavenumber. The value of δ is the field decrease factor. The coordinate system is shown in Fig. 1. As a special case, the field on the undulator middle plane (y=0) can be expressed as:

$$B_y = -B_0(1-\kappa x^2)\sin(k_u z). \tag{1}$$

Where $\kappa=\delta\dfrac{k_u^2}{4}$.

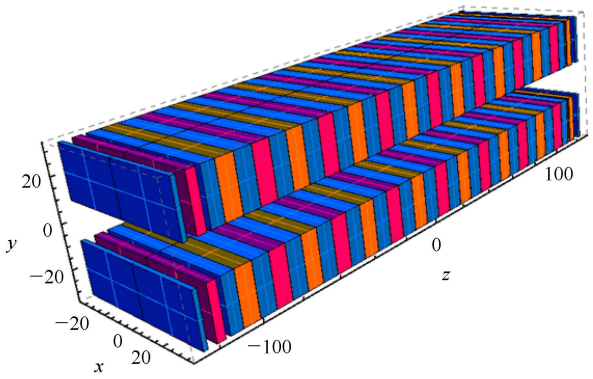

Fig. 1. An idealized HUST-FEL undulator modeled with RADIA [12]. The z-axis is the direction of radiation and the x-axis is the direction of electron swing.

2.2 Derivation of the beam transfer matrices of the planar undulator

2.2.1 Horizontal plane

Based on the magnetic field distribution (1), the Lorentz force in the x-axis direction can be expressed as:

$$f_x \approx -ev_z B_y \approx e\beta cB_0\sin(k_u z) - e\beta cB_0\kappa x^2\sin(k_u z).$$

Since $v_z \gg v_y$, the force $ev_y B_z$ is neglected and the equation of the electronic motion in the x-axis direction is simplified as

$$(\gamma m_e)\frac{\mathrm{d}^2x}{\mathrm{d}t^2} = (\gamma m_e)(\beta c)^2\frac{\mathrm{d}^2x}{\mathrm{d}z^2} = f_x. \tag{2}$$

Where, Eq. $z\approx\beta ct$ has been taken.

Generally, the pole width of the undulator is designed to be so wide that a large good field region can be guaranteed for the beam traveling through. It turns out that the field attenuation (κx^2) should be a tiny value. Therefore, the differential Eq. (2) can be solved by a perturbation method with a result of 0-order approximate solution where the last item of the equation is neglected.

$$x^{(0)}(z) = x_0 + x_0' z - \frac{\sqrt{2}a_u}{\gamma k_u}\sin(k_u z). \tag{3}$$

Where a_u is known as the RMS undulator constant and γ is the Lorentz factor. The 1st-order approximate solution can be obtained by taking (3) back to the equation:

$$x^{(1)}(z) = x^{(0)}(z) + \frac{1}{3}\frac{a_u^2\kappa}{\gamma^2\beta}(3x_0 + x_0' z)z^2. \tag{4}$$

In solution (4), all small oscillating items are neglected.

First, if the 0-order solution is considered for electron motion, the transfer matrix is

$$M_x^{(0)} = \begin{pmatrix} 1 & z \\ 0 & 1 \end{pmatrix}. \tag{5}$$

This result implies that the undulator magnetic field has no obvious effect on the beam and it acts just as a segment drift space at the x-axis direction.

Second, if the 1st-order solution is considered as the orbit electron, the beam transfer matrix becomes:

$$M_x^{(1)} = \begin{pmatrix} 1+\dfrac{a_u^2\kappa}{\gamma^2\beta}z^2 & z+\dfrac{1}{3}\dfrac{a_u^2\kappa}{\gamma^2\beta}z^3 \\ 2\dfrac{a_u^2\kappa}{\gamma^2\beta}z & 1+\dfrac{a_u^2\kappa}{\gamma^2\beta}z^2 \end{pmatrix}. \tag{6}$$

It can be inferred from matrix (6) that an undulator's magnetic field has a weak nonlinear defocus effect on the beam. This effect will be enlarged for low energy beam and longer undulator. In addition, the defocus effect is proportional to the field decrease factor κ.

2.2.2 Vertical plane

The motion equation of the well-known betatron oscillation in the regular period region of undulator is [13]

$$\left(\frac{\mathrm{d}^2}{\mathrm{d}z^2}+k_y\right)y = 0.$$

Where $k_y = a_u k_u/\gamma$ and it is the wavenumber of the beta oscillation. The beam transport matrix in the y-axis direction is

$$M_y = \begin{pmatrix} \cos(k_y z) & \dfrac{1}{k_y}\sin(k_y z) \\ -k_y\sin(k_y z) & \cos(k_y z) \end{pmatrix}. \tag{7}$$

The end part of the undulator has an effect on the beam as well. In general, the end part of the undulator is very short, and its influence on the beam can be equivalent to a FODO (focusing-drift-defocusing-drift) structure [14].

The vertical Lorentz force can be expressed as

$$f_y \approx -eB_z v_x \sim Q_y(z)y.$$

Where $Q_y(z)$ is the focus coefficient.

As shown in Fig. 2, the distribution of the focus coefficient of the undulator in HUST-FEL is calculated a numerical method, and the fringe field plays a defocusing role while the end part of the field plays a focusing role. The undulator equivalent transfer line is showed in Fig. 3. Based on the principle of equivalent effect, the transfer matrix of the end part can be given by:

$$M_{\rm D}=\begin{pmatrix} 1 & 0 \\ \dfrac{1}{0.0048\gamma^2} & 1 \end{pmatrix},\quad M_{\rm F}=\begin{pmatrix} 1 & 0 \\ -\dfrac{1}{0.154\gamma^2} & 1 \end{pmatrix},$$

$$M_{\rm O}=\begin{pmatrix} 1 & 0.033 \\ 0 & 1 \end{pmatrix}.$$

In addition, there is a 0.1 m-long drift space at both ends of the undulator. So, the transport matrix of the end part is:

$$M=\begin{pmatrix} 1 & 0.1 \\ 0 & 1 \end{pmatrix} M_{\rm D}M_{\rm O}M_{\rm F}.$$

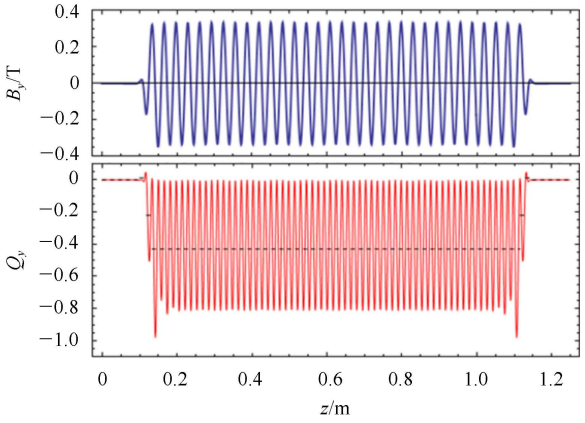

Fig. 2. Distribution of the magnetic field on-axis (upper) and the focus force coefficient (bottom). The focus force coefficient is normalized. The dashed line presents the average focus coefficient of each segment.

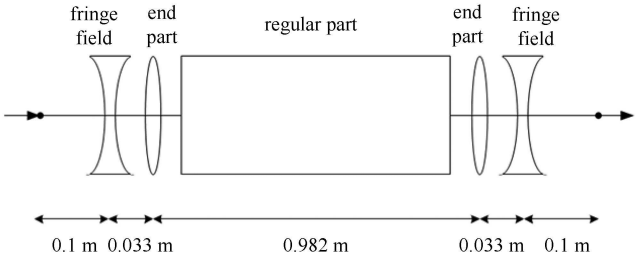

Fig. 3. The undulator in HUST-FEL equivalent transfer line (vertical plane). From 0.1 m in front of the undulator to 0.1 m behind it is studied in this paper. The effect of the fringe field and the end part of the field can be equal to a defocusing and focusing lens.

Till then, the beam transfer matrices of the undulator are obtained completely. Based on them, optimization of the lattice function will be discussed in the next section.

3 Optimization of lattice function

The purpose of lattice function optimization is to look for an appropriate beta function to decrease the gain length of the FEL, which is primarily related to the average value of the beta function [9, 15, 16]. As well, a smaller beta function will contribute to a higher average current density and an equivalent energy spread of the electron beam [8, 15]. Owing to the fact that the particles in the beam all have different betatron oscillation amplitudes, one obtains a fact not only a reduction in the longitudinal speed but in addition, a smear which is equivalent to the energy spread of the incident beam occurs [8, 17].

$$(\sigma_\eta)_{\rm eq}\approx\frac{\gamma^2\varepsilon}{\beta_{\rm avg}}.$$

Furthermore, the fill factor $\sigma_{\rm A}$ which describes the relative overlap of the electron beam and the radiation field has a relation with the beta function [18, 19]

$$\sigma_{\rm A}\approx\begin{cases}\dfrac{S_{\rm opt}}{S_{\rm beam}} & S_{\rm opt}<S_{\rm beam}\\ \dfrac{S_{\rm beam}}{S_{\rm opt}} & S_{\rm opt}\geqslant S_{\rm beam}\end{cases}.$$

Radiation diffraction possess a dominant factor in gain length growth especially for long wavelength FELs, due to comparable values between the beam cross section and the radiation wavelength. Xie has presented the

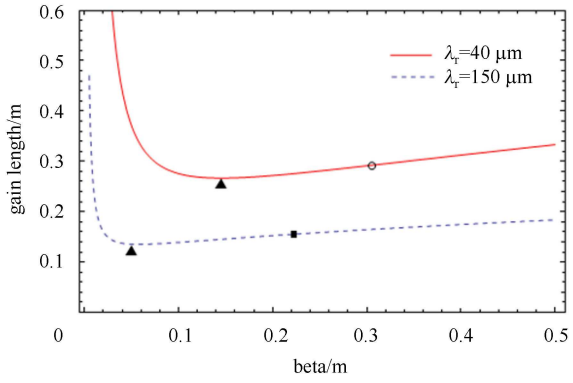

Fig. 4. (color online) Gain length versus the average beta function for different radiation wavelengths. The best value is about 0.15 m ($\lambda_{\rm r}$= 40 μm) and 0.06 m ($\lambda_{\rm r}$=150 μm). They are marked with a black triangle. The minimum average beta function value with natural focusing is about 0.31 m ($\lambda_{\rm r}$=40 μm) and 0.22 m ($\lambda_{\rm r}$= 150 μm). They are marked with a circle and a black square.

theory of 3D gain length, which includes the influence of the parameters of energy spread, diffraction and angular spread [6].

For the HUST-FEL, the FEL simulation result based on the Xie formula is shown in Fig. 4. It implies that the best average beta function is about 0.15 m (λ_r= 40 μm) and 0.06 m (λ_r=150 μm). Too large or too small value will lead to an increase of the gain length. So the approach of optimization of the beta function is to adjust the initial Twiss parameter aiming at the optimal value of the beta function. In addition, the general principle for beam matching should be considered too. 1) Beam waist should be achieved at the center of the undulator, with a symmetrical distribution of the beta function for both directions; 2) minimum values of beta function and small fluctuation within the undulator for strongly focusing vertical direction. The maximum beta function should not be too large as well.

3.1 Horizontal plane

Set the initial Twiss parameter of the x-axis direction as

$$\Sigma_{x0}=\begin{pmatrix}\gamma_{x0} & \alpha_{x0}\\ \alpha_{x0} & \beta_{x0}\end{pmatrix}.$$

When using the 0-order approximate solution, according to Eq. (5), the beta function of the x-axis direction can be expressed as

$$\beta_x(z)=\gamma_{x_0}z^2-2\alpha_{x_0}z+\beta_{x_0}.$$

The average beta function of (0, z_m) is

$$\overline{\beta_x}=\frac{1}{3}\gamma_{x0}z_m^2-\alpha_{x0}z_m+\beta_{x0}.$$

Where z_m is the transfer line length.

When the initial condition is

$$\alpha_{x0}=\sqrt{3},\quad \beta_{x0}=2z_m/\sqrt{3}, \tag{8}$$

the average beta function $\overline{\beta_x}$ reaches the minimum value $z_m/\sqrt{3}$. If the optimization object is that the maximum of the beta function reaches the minimum value, the initial condition should be

$$\alpha_{x0}=1,\quad \beta_{x0}=z_m.$$

Under this condition, the average beta function is $2z_m/3$ and the maximum of the beta function is z_m. The beta function curves for both cases are shown in Fig. 5.

3.2 Vertical plane

In the same way as with the horizontal plane, we set the initial Twiss parameter of the vertical plane as

$$\Sigma_{y0}=\begin{pmatrix}\gamma_{y0} & \alpha_{y0}\\ \alpha_{y0} & \beta_{y0}\end{pmatrix}.$$

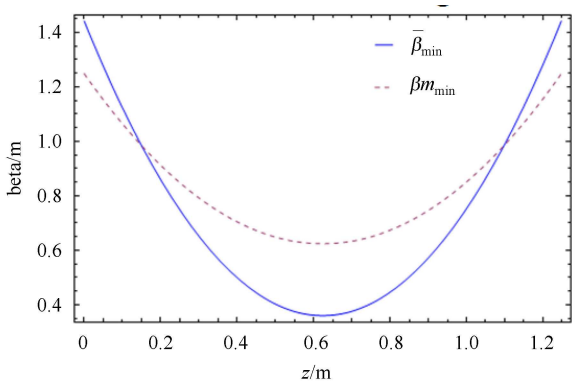

Fig. 5. (color online) Continuous line: beta function curves of optimization $\overline{\beta}_{\min}$ (minimize the average beta function). Dashed line: beta function curves of optimization $\beta m_{\min}$ (minimize the maximum beta function).

Based on Eq. (7), the beta function of the beam in the vertical plane can be presented as

$$\beta_y(z)=\left(\frac{\beta_{y0}}{2}+\frac{\gamma_{y0}}{2k_y^2}\right)+\sqrt{\left(\frac{\beta_{y0}}{2}-\frac{\gamma_{y0}}{2k_y^2}\right)^2+\left(\frac{\alpha_{y0}}{k_y}\right)^2}\sin[2k_yz+\varphi].$$

Where the initial phase satisfies the equation:

$$\varphi=\arctan\left(-\frac{\beta_{y0}k_y^2-\gamma_{y0}}{2\alpha_{y0}k_y}\right).$$

Hence, the average beta function is

$$\overline{\beta_y}=\left(\frac{\beta_{y0}}{2}+\frac{\gamma_{y0}}{2k_y^2}\right).$$

When the initial condition is

$$\alpha_{y0}=0,\quad \beta_{y0}=1/k_y \tag{9}$$

the average beta function reaches the minimum value $1/k_y$. At the same time, the beta function equals a constant.

The maximum value of the beta function is

$$\beta_{y\max}=\left(\frac{\beta_{y0}}{2}+\frac{\gamma_{y0}}{2k_y^2}\right)+\sqrt{\left(\frac{\beta_{y0}}{2}-\frac{\gamma_{y0}}{2k_y^2}\right)^2+\left(\frac{\alpha_{y0}}{k_y}\right)^2}.$$

With the same initial condition, the maximum value of the beta function reaches the minimum value also.

Based on the lattice analysis of the vertical and horizontal plane, the minimum average beta function of the beam can be expressed as:

$$\overline{\beta}=\sqrt{\overline{\beta_x}\ \overline{\beta_y}}=\sqrt{\frac{N_u\lambda_u}{\sqrt{3}}\frac{\gamma}{a_uk_u}}. \tag{10}$$

Based on Eq. (10), the minimum average beta function is about 0.31 m and 0.22 m when the beam energy

is 12 MeV (λ_r=40 μm,) and 6 MeV (λ_r=150 μm). They are larger than the best value calculated by Xie Ming's formula. Instead of the initial condition (8) and (9), the average beta function will be larger and the gain length increases too. So they will be selected as the optimized initial Twiss parameter.

The optimal Twiss parameter at the start of the regular part is shown in Eq. (9), which has been obtained, and thus

$$\Sigma_u = \begin{pmatrix} k_y & 0 \\ 0 & \dfrac{1}{k_y} \end{pmatrix}.$$

So the Twiss parameter at 0.1 m in the front undulator can be calculated by Eq. (11)

$$\Sigma_{\rm st} = M\Sigma_u M^{\rm T}. \tag{11}$$

4 Numerical simulations

In order to verify the accuracy of the results obtained by the theoretical calculation from the derived transfer matrix, a code was written to calculate the motion of beams in the 3D magnetic field. If the field decrease factor is κ=30/m^2 and the beam energy is 6 MeV, the beta function in the x-axis direction curves of 0-order and 1$^{\rm st}$-order approximation, as well as the numerical solution, are shown in Fig. 6. The numerical result has been validated by another code PTP [20]. Compared with 0-order, the beta function obtained by 1$^{\rm st}$-order is more consistent with that obtained by the numerical method. Clearly illustrating the beta functions calculated by three different methods at the point which is 0.1 meter away from the exit of the undulator, are listed in Table 2. In spite of 0-order transfer matrix imprecision, it can be used to calculate and optimize the lattice unless the field decreasing factor is too large.

Table 2. The beta functions at the point which is 0.1 m away from the exit of the undulator calculated by different methods.

method	numerical	0-order	1$^{\rm st}$-order
$\beta_{x\rm out}$	1.347	1.248	1.337

When the beam energy is 6 MeV or 12 MeV, the Twiss parameter at 0.1 m in front of the undulator can be calculated based on Eq. (11).

$$\Sigma_{\rm st-6} = \begin{pmatrix} 11.06 & 1.357 \\ 1.357 & 0.257 \end{pmatrix}$$

$$\Sigma_{\rm st-12} = \begin{pmatrix} 5.698 & 0.6980 \\ 0.6980 & 0.2610 \end{pmatrix}.$$

The curves of the beta function in the two cases are shown in Fig. 7. They are both compared with the result calculated by a numerical method too. The results by analytical method in this paper and numerical method are matched well. It is shown that the method in this paper has high precision.

For beam energy in the region from 6 MeV to 12 MeV, the beta functions calculated by the analytical method are shown in Fig. 8.

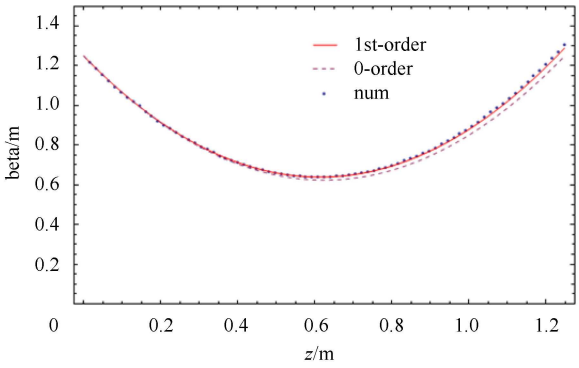

Fig. 6. (color online) The beta function in the horizontal plane curves of 0-order, 1st-order approximation and numerical solution.

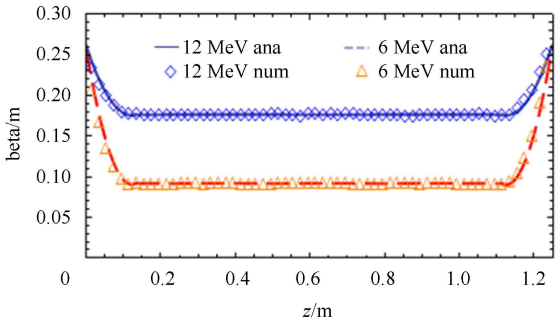

Fig. 7. (color online) The curves of beta function calculated by transfer matrix and numerical method when the beam energy is 6 MeV and 12 MeV.

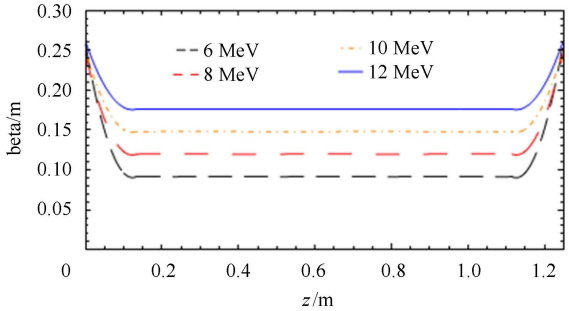

Fig. 8. (color online) The beta functions calculated by transfer matrix for beam energy from 6 MeV to 12 MeV.

5 Conclusions and discussions

The result calculated by the analytical method presented in this paper matches well with the numerical method; this method is efficient for designing and optimizing the lattice of the long wavelength FEL. The average beta functions obtained by this method can be taken as eigenvalues to analyze the gain length and the small signal gain of FEL. Besides, in a short wavelength FEL, the focus or defocus force is weak in both the horizontal and vertical direction due to the high beam energy. The beam transport characteristics in two planes are closer to the drift space. So, the method in this paper is not suitable to design the lattice of a short wavelength FEL.

The expressions of the average beta function can be regarded as optimal values and used to optimize other parameters of FEL, such as undulator period, undulator constant and so on.

In addition, the beam emittance increase in the horizontal plane derived from non-linear defocusing need be considered in an infrared FEL project. For HUST-FEL, its field decrease factor is about κ=30/m^2 [10]. When the radiation wavelength is 0.3 mm, based on Eq. (6), the magnitude of the emittance growth is about 10^{-2}. In order to ensure that the emittance does not exceed the limitation of $\lambda_r/4\pi$, the decrease factor must be considered. When more precise calculation of the gain length is demanded, the emittance growth needs to be considered as well.

The physical design of the HUST-FEL undulator was accomplished [10]. We signed a contract with Kyma s.r.l., for the magnet design and manufacturing of this planar PPM undulator; the final assemble with performance test is expected to be finished at the end of 2013.

References

1 Krinsky S. The Physics and Properties of Free-Electron Lasers. AIP Conference Proceedings. 2002, **648**: 23
2 HUANG Z, Kim K J. Physical Review Special Topics-Accelerators and Beams, 2007, **10**(3): 034801
3 Feldhaus J, Arthur J, Hastings J B. Journal of Physics B: Atomic, Molecular and Optical Physics, 2005, **38**(9): S799
4 Pellegrini C, Stöhr J. Nuclear Instruments and Methods in Physics Research Section A: Accelerators, Spectrometers, Detectors and Associated Equipment, 2003, **500**(1): 33–40
5 Saldin E L, Schneidmiller E E A, Yurkov M V. The Physics of Free Electron Lasers. Springer Verlag, 2000
6 XIE M. Design Optimization for an X-ray Free Electron Laser Driven by SLAC Linac Particle Accelerator Conference, 1995, Proceedings of the 1995. IEEE, 1995, **1**: 183–185
7 Nuhn H D. Linac Coherent Light Source (LCLS) Conceptual Design Report. Stanford Linear Accelerator Center, Menlo Park, CA (US), 2002
8 Schmüser P, Dohlus M, Rossbach J. Ultraviolet and Soft X-ray Free-Electron Lasers: Introduction to Physical Principles, Experimental Results, Technological Challenges. Springer Verlag, 2008
9 Qi-ka J, Shancai Z, Shengkuan L et al. Design of Undulator for the Shanghai DUV-FEL Proceedings of the 2004 FEL Conference. 2004, 494–497
10 QIN B, TAN P, YANG L, LIU X L. Nuclear Instruments and Methods in Physics Research A, 2013, **727**: 90–96
11 Quattromini M, Artioli M, Di Palma E et al. Physical Review Special Topics-Accelerators and Beams, 2012, **15**(8): 080704
12 RADIA Technical Reference Manual. ESRF, Grenoble, France
13 Freund H P, Antonsen T M. Principles of Free-Electron Lasers. Springer Verlag, 1996
14 Wiedemann H. Particle Accelerator Physics. Springer Verlag, 2007
15 Emma P, HUANG Z, Kim K J et al. Physical Review Special Topics-Accelerators and Beams, 2006, **9**(10): 100702
16 Zholents A A. Physical Review Special Topics-Accelerators and Beams, 2005, **8**(4): 040701
17 HUANG Z, Borland M, Emma P et al. Physical Review Special Topics-Accelerators and Beams, 2004, **7**(7): 074401
18 Freund H P, Neil G R. Proceedings of the IEEE, 1999, **87**(5): 782–803
19 DOU Y, SHU X, WANG Y. High Power Laser and Particle Beams, 2006, **8**: 024 (in Chinese)
20 QIN B, CHEN D Z, ZHAO L C et al. Nuclear Instruments and Methods in Physics Research Section A: Accelerators, Spectrometers, Detectors and Associated Equipment, 2010, **620**(2): 121–127